(q, ^3J=3.2 Hz, SiH, 1H), 7.27-7.61 ppm (m, $C_6\underline{H_4}Me$, 4H). ^{13}C NMR ($CDCl_3$, 125 MHz): 19.37 ppm, 21.71 ppm, 22.93 ppm, 23.14 ppm, 129.00 ppm, 130.99 ppm, 132.34 ppm, 134.71 ppm, 139.62 ppm. Mass (m/z, relative intensity): 202 (56, M^+), 187 (11), 159 (13), 121 (10), 110 (100), 95 (36), 67 (16).

7. (*o*-Tolyl)silane (**11a**): ^1H NMR (C_6D_6, 500 MHz): 2.20 ppm (s, $C_6H_4\underline{Me}$, 3H), 4.24 ppm (s, SiH_3, 3H), 6.93-7.46 ppm (m, $C_6\underline{H_4}Me$, 4H). Mass (m/z, relative intensity): 122 (63, M^+), 119 (22), 105 (26), 91 (100), 77 (6), 67 (9), 53 (12).
(*m*-Tolyl)silane (**11b**): ^1H NMR (C_6D_6, 500 MHz): 2.37 ppm (s, $C_6H_4\underline{Me}$, 3H), 4.20 ppm (s, SiH_3, 3H), 7.23-7.43 ppm (m, $C_6\underline{H_4}Me$, 4H). Mass (m/z, relative intensity): 122 (78, M^+), 105 (23), 93 (19), 91 (100), 67 (7), 53 (9), 42 (5).
(*p*-Tolyl)silane (**11c**): ^1H NMR (C_6D_6, 500 MHz): 2.39 ppm (s, $C_6H_4\underline{Me}$, 3H), 4.22 ppm (s, SiH_3, 3H), 7.22 ppm (d, ^3J=7.8 Hz, $C_6\underline{H_4}Me$, 2H), 7.52 ppm (d, ^3J=7.7 Hz, $C_6\underline{H_4}Me$, 2H). Mass (m/z, relative intensity): 122 (54, M^+), 105 (20), 91 (100), 90 (8), 67 (9), 65 (19), 53 (20), 39 (12).
1,2-Benzo-3-sila-1-cyclobutene (**12a**): ^1H NMR (C_6D_6, 80 MHz): 2.23 ppm (t, ^3J=4 Hz, CH_2, 2H), 4.63 ppm (t, ^3J=4.8 Hz, SiH_2, 2H), 6.69-7.07 ppm (m, C_6H_4, 4H). Mass (m/z, relative intensity): 120 (100, M^+), 106 (3), 105 (80), 93 (29), 79 (4), 77 (7), 66 (11), 53 (16).
Bis(*m*-tolyl)silane (**13b**): ^1H NMR (C_6D_6, 500 MHz): 2.05 ppm (s, $C_6H_4\underline{Me}$, 3H), 5.16 ppm (s, SiH_2, 2H), 7.00-7.44 ppm (m, $C_6\underline{H_4}Me$, 4H). Mass (m/z, relative intensity): 212 (40, M^+), 195 (3), 134 (5), 120 (100), 104 (53), 93 (16), 912 (12), 67 (4), 53 (6).

8. 1,1,1-Triethyl-2-(*m*-tolyl)disilane (**5b**): ^1H NMR (C_6D_6, 500 MHz): 0.68 ppm (q, ^3J=7.9 Hz, $SiCH_2\underline{CH_3}$, 6H), 0.98 ppm (t, ^3J=7.8 Hz, $SiCH_2\underline{CH_3}$, 9H), 2.11 ppm (s, $C_6H_4\underline{Me}$, 3H), 4.45 ppm (s, SiH_2, 2H), 6.98-7.46 ppm (m, $C_6\underline{H_4}Me$, 4H). Mass (m/z, relative intensity): 236 (17, M^+), 207 (4), 179 (9), 151 (22), 115 (100), 87 (85), 59 (18), 43 (3).
1,1,1-Triethyl-2-(*p*-tolyl)disilane (**5c**): ^1H NMR (C_6D_6, 500 MHz): 0.67 ppm (q, ^3J=7.9 Hz, $SiCH_2CH_3$, 6H), 0.98 ppm (t, ^3J=8.0 Hz, $SiCH_2\underline{CH_3}$, 9H), 2.08 ppm (s, $C_6H_4\underline{Me}$, 3H), 4.46 ppm (s, SiH_2, 2H), 7.00-7.53 ppm (m, $C_6\underline{H_4}Me$, 4H). Mass (m/z, relative intensity): 236 (20, M^+), 207 (4), 179 (10), 151 (24), 115 (100), 87 (90), 59 (22), 53 (4).

9. Steele, K. P.; Tzeng, D.; Weber, W. P. *J. Organomet. Chem.* **1982**, *231*, 291-298.

10. Dimethoxy(*o*-tolyl)silane (**6a**): ^1H NMR (C_6D_6, 500 MHz): 2.47 ppm (s, $C_6H_4C\underline{H_3}$, 3H), 3.40 ppm (s, SiOMe, 6H), 5.17 ppm (s, SiH, 1H), 6.97-7.79 ppm (m, $C_6\underline{H_4}CH_3$, 4H). Mass (m/z, relative intensity): 182 (14, M^+), 152 (2), 151 (5), 119 (4), 105 (4), 91 (100), 77 (3), 61 (41).
Dimethoxy(*m*-tolyl)silane (**6b**): Mass (m/z, relative intensity): 182 (52, M^+), 181 (64), 151 (22), 133 (2), 121 (10), 91 (100), 77 (3), 59 (39), 45 (4).
Trimethoxy(*o*-tolyl)silane (**7a**): Mass (m/z, relative intensity): 212 (15, M^+), 180 (8), 165 (4), 150 (7), 121 (100), 92 (11), 91 (99), 59 (30).
Trimethoxy(*m*-tolyl)silane (**7b**): Mass (m/z, relative intensity): 212 (33, M^+), 181 (20), 167 (3), 151 (8), 120 (100), 91 (58), 59 (20), 45 (3).
Trimethoxy(*p*-tolyl)silane (**7c**): Mass (m/z, relative intensity): 212 (24, M^+), 181 (14), 151 (8), 123 (3), 120 (100), 90 (59), 59 (20), 45 (3).
Methoxybis(*m*-tolyl)silane (**8b**): Mass (m/z, relative intensity): 242 (10, M^+), 211 (6), 179 (2), 150 (100), 119 (12), 105 (21), 65 (5), 59 (45).
Methoxybis(*p*-tolyl)silane (**8c**): Mass (m/z, relative intensity): 242 (14, M^+), 211 (14), 179 (2), 150 (100), 119 (10), 105 (5), 91 (8), 59 (18).
Dimethoxybis(*m*-tolyl)silane (**9b**): Mass (m/z, relative intensity): 272 (20, M^+), 241 (4), 183 (10), 181 (100), 151 (27), 105 (36), 91 (13), 59 (22).
Dimethoxybis(*p*-tolyl)silane (**9c**): Mass (m/z, relative intensity): 272 (22, M^+), 241 (4), 211 (4), 181 (100), 151 (23), 121 (23), 91 (9), 59 (14).

Unusual Effect of the Connecting Tether Direction of a Liquid Chromatographic Chiral Stationary Phase on the Chiral Recognition

Myung Ho Hyun*, Chung-Sik Min, and Kyung Kyu Jyung†

Department of Chemistry, Pusan National University, Pusan 609-735, Korea
†*Department of Chemistry Education, Pusan National University, Pusan 609-735, Korea*

Received December 31, 1995

Subtle structural changes of Pirkle-type chiral stationary phases (CSPs) for the liquid chromatographic resolution of enantiomers have been known to show often remarkable influences on enantioselectivity. For example, increasing the π-basicity of the aryl functionality of π-basic Pirkle-type CSPs or changing the conformational rigidity of CSPs has affected their enantioselectivities.[1] The manner of connecting a chiral selector to solid column support has been another important factor influencing the degree of enantioselectivity.[2] Especially, the direction and the length of the connecting tether of Pirkle-type CSPs have been engineered to manipulate the resolution trends for resolving a homologous series of racemic analytes in elucidating the chiral recognition mechanism or to enhance the enantioselectivity.[3]

In this study, we prepared a new CSP (**1**) by bonding N-(3,5-dinitrobenzoyl)-(R)-4-hydroxyphenylglycine to silica gel through the 4-hydroxy functionality.[4] CSP **1** maintains the integrity of the structure of a representative commercial π-acidic CSP (**2**) derived from N-(3,5-dinitrobenzoyl)-(R)-phenylglycine except the direction of the connecting tether. To elucidate the characteristics of CSP **1**, we resolved various racemic α-amino acid derivatives on CSP **1** and compared the resolution results with those on CSP **2**. We consequently found there are drastic discrepancies between the chromatographic resolving ability of CSP **1** and **2** for the two enantio-

Table 1. Comparison of the resolution of π-acidic N-(3,5-dinitrobenzoyl) derivatives **3** and **4** on CSP **1** and CSP **2**[a]

Analyte[b]	R	Y	CSP 1			CSP 2		
			k_1'[c]	α[d]	Configuration[e]	k_1'[c]	α[d]	Configuration[e]
3a	CH_3	CH_2CH_3	12.60	1.54	S	18.58	1.00	
b	$CH(CH_3)_2$	CH_2CH_3	10.36	1.88	S	13.83	1.00	
c	$CH_2CH(CH_3)_2$	CH_3	10.56	2.08	S	14.47	1.22	S
d	$CH_2CH(CH_3)_2$	CH_2CH_3	8.60	2.13	S	10.94	1.10	S
e	$CH_2CH(CH_3)_2$	$(CH_2)_3CH_3$	7.17	2.36	S	8.98	1.00	
f	$CH_2CH(CH_3)_2$	$(CH_2)_7CH_3$	5.63	2.77	S	6.60	1.00	
g	$CH_2CH(CH_3)_2$	$(CH_2)_9CH_3$	5.00	2.90	S	5.85	1.00	
h	$(CH_2)_2CH_3$	CH_2CH_3	9.83	1.92		12.53	1.05	
i	$(CH_2)_4CH_3$	CH_2CH_3	9.11	2.08		10.32	1.10	
j	$(CH_2)_6CH_3$	CH_2CH_3	8.23	2.16		8.76	1.13	
k	$(CH_2)_7CH_3$	CH_2CH_3	7.98	2.24		8.52	1.15	
l	$(CH_2)_9CH_3$	CH_2CH_3	7.44	2.41		7.59	1.15	
m	Phenyl	CH_2CH_3	19.05	1.57	S	23.57	1.00	
n	Benzyl	CH_2CH_3	18.31	1.82		22.20	1.00	
4a	CH_3	$(CH_2)_2CH_3$	3.74	4.03	S	5.92	1.22	S
b	$CH(CH_3)_2$	$(CH_2)_2CH_3$	2.70	6.16	S	3.20	1.58	S
c	$CH_2CH(CH_3)_2$	$(CH_2)_2CH_3$	3.03	6.23	S	3.01	1.52	S
d	Phenyl	$(CH_2)_2CH_3$	5.98	3.72	S	6.88	1.42	S
e	Benzyl	$(CH_2)_2CH_3$	6.72	5.26		6.58	1.52	

[a]Chromatography was performed with a system consisting of a Waters Model 510 pump, a Rheodyne Model 7125 Injector with a 20 μL sample loop, a Youngin Model 710 Absorbance Detector and a Youngin D520B Computing Integrator. Data for **3a** and **4a** were obtained respectively using 10% and 20% isopropyl alcohol in *n*-hexane as a mobile phase with flow rate of 2 mL/min at 254 nm UV. [b]Racemic analytes resolved on CSP **1**. [c]Capacity factors. [d]Separation factors. [e]Absolute configuration of the second eluted enantiomer. For blanks, the elution orders have not been established.

mers of π-acidic racemates.[5]

Table 1 summarizes the results for resolving π-acidic N-(3,5-dinitrobenzoyl) derivatives of α-amino esters **3** and α-amino amides **4** on CSP **1** and **2**. Typical chromatograms for resolving racemic leucine derivative **4c** on CSP **1** and **2** are presented in Figure 1. As shown in Table 1 and Figure 1, CSP **1** resolves π-acidic racemates surprisingly well while CSP **2** does not. Particularly, CSP **1** shows excellent enantioselectivities for the N-(3,5-dinitrobenzoyl) derivatives of α-amino amides (**4**). The results summarized in Table 1 are very interesting in that CSP **1**, which contains 3,5-dinitrobenzoyl group and thus is considered to be π-acidic, can resolve π-acidic analytes with quite large separation factors.

Pirkle-type CSPs have been known to require an effective π-π donor acceptor interaction between the CSP and the analyte for the effective enantioseparation.[6] For the utilization of effective π-π donor acceptor interaction between the CSP and the analyte, π-acidic CSPs have been used to resolve π-basic racemates[7] and, similarly, π-basic CSPs have been used to resolve π-acidic racemates.[8] In this context, the high enantioselectivities exerted by CSP **1** for resolving π-acidic racemates shown in Table 1 are unexpected because CSP **1** is not anticipated to induce an effective π-π donor acceptor interaction with π-acidic racemates. The resolution of π-acidic racemates on other π-acidic CSPs has already been claimed by several workers including authors.[9] However, the chromatographic resolution results listed in Table 1 for the two enantiomers of π-acidic racemates are most significant.

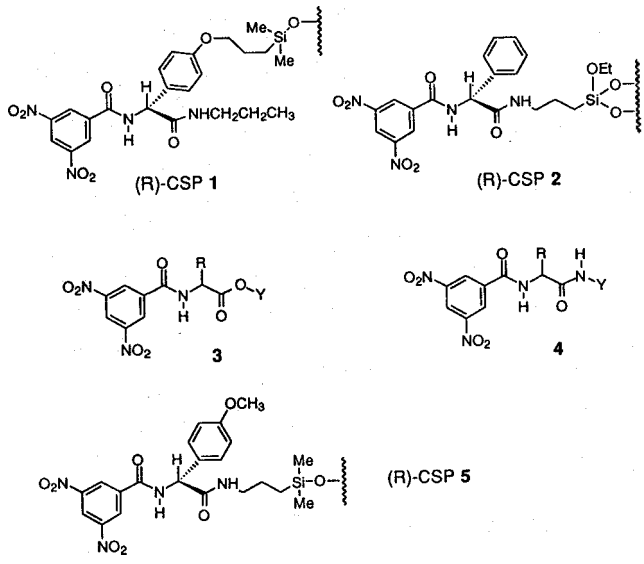

The origin of the greater enantioselectivities for the π-acidic racemates on CSP **1** than on CSP **2** might be considered to stem from two factors. The one is the direction of the connecting tether and the other is the greater π-basicity of the *p*-alkoxyphenyl group of CSP **1** than that of the simple phenyl group of CSP **2**. The increased π-basicity of the *p*-alkoxyphenyl group of CSP **1** compared to that of the simple phenyl group of CSP **2** may induce an effective π-π donor

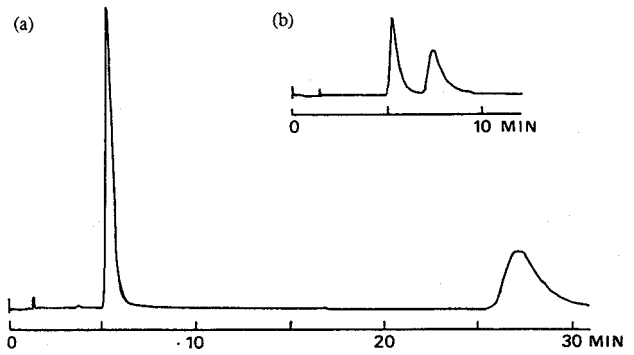

Figure 1. Chromatograms for resolving **4c** on (a) CSP **1** and on (b) CSP **2**. For chromatographic conditions, see the footnote to Table 1.

acceptor interaction with π-acidic racemates. The effect of the increased π-basicity of the *p*-alkoxyphenyl group of CSP **1** on the enantioselectivities for the two enantiomers of π-acidic racemates may be considered separately from that of the direction of connecting tether by preparing CSP **5**.[4] The direction of the connecting tether of CSP **5** is the same as that of CSP **2** and, consequently, the chromatographic resolution results on CSP **5** is expected to show only the effect of the increased π-basicity of the *p*-alkoxyphenyl group of the CSP. Based on this rationale, CSP **5** was prepared[4] and used in resolving π-acidic racemates. The chromatographic resolution results on CSP **5** are summarized in Table 2. The data in Table 2 show that the enantioselectivities on CSP **5** are a little greater than those on CSP **2** but much worse than those on CSP **1**. These results indicate that the greater enantioselectivities for the two enantiomers of the π-acidic racemates on CSP **1** than on CSP **2** stem somewhat from the increased π-basicity of the *p*-alkoxyphenyl group of CSP **1** and quite largely from the different direction of the connecting tether of CSP **1**.

As an effort to see the effect of the direction of the connecting tether of CSP **1** on the chiral recognition, we examined the resolution trends of a series of N-(3,5-dinitrobenzoyl) leucine alkyl esters (**3c-g**) and N-(3,5-dinitrobenzoyl)-α-alkylglycine ethyl esters (**3a, 3h-l**) on CSP **1** and found that the separation factors (α) increase continuously as the ester alkyl tail or the alkyl tail at the chiral center of the analytes increases in length as shown in Table 1. However, the separation factors (α) for resolving N-(3,5-dinitrobenzoyl) leucine alkyl esters (**3c-g**) on CSP **2** and **5** decrease continuously as the ester alkyl tail of the analytes increases in length while those for resolving N-(3,5-dinitrobenzoyl)-α-alkylglycine ethyl esters (**3a, 3h-l**) on CSP **2** and **5** increase continuously as the alkyl tail at the chiral center of the analytes increases in length as shown in Table 2 and 3. Those somewhat complicated chiral recognition trends cause our effort to elucidate the role of the connecting tether direction of CSPs in the chiral recognition from the study of CPK molecular models unsuccessful.

In conclusion, CSP **1**, which maintains the integrity of the structure of CSP **2** except the direction of the connecting tether, has shown much greater enantioselectivities than CSP **2** for the two enantiomers of π-acidic N-(3,5-dinitrobenzoyl)-α-amino esters and amides. At the present time, we speculate that the significantly enhanced chiral recognition ability of CSP **1** compared to that of CSP **2** may stem mainly from the different direction of the connecting tether of the CSP. However, the details about the chiral recognition mechanism including the role of the direction of the connecting tether in the chiral recognition are not yet clear. Efforts to elucidate the more details of the chiral recognition mechanism are under way in our laboratory.

Table 2. Resolution of π-acidic N-(3,5-dinitrobenzoyl) derivatives **3** and **4** on CSP **5**.[a]

Analyte[b]	R	Y	k_1'[c]	α[d]	Configuration[e]
3a	CH_3	CH_2CH_3	8.85	1.08	S
b	$CH(CH_3)_2$	CH_2CH_3	8.37	1.09	S
c	$CH_2CH(CH_3)_2$	CH_3	7.70	1.35	S
d	$CH_2CH(CH_3)_2$	CH_2CH_3	6.63	1.27	S
e	$CH_2CH(CH_3)_2$	$(CH_2)_3CH_3$	5.68	1.15	S
f	$CH_2CH(CH_3)_2$	$(CH_2)_7CH_3$	4.60	1.05	S
g	$CH_2CH(CH_3)_2$	$(CH_2)_9CH_3$	4.06	1.00	
h	$(CH_2)_2CH_3$	CH_2CH_3	7.45	1.19	
i	$(CH_2)_4CH_3$	CH_2CH_3	6.21	1.25	
j	$(CH_2)_6CH_3$	CH_2CH_3	5.36	1.29	
k	$(CH_2)_7CH_3$	CH_2CH_3	5.12	1.33	
l	$(CH_2)_9CH_3$	CH_2CH_3	4.64	1.36	
m	Phenyl	CH_2CH_3	13.28	1.00	
n	Benzyl	CH_2CH_3	18.65	1.00	
4a	CH_3	$(CH_2)_2CH_3$	3.48	1.62	S
b	$CH(CH_3)_2$	$(CH_2)_2CH_3$	2.63	2.12	S
c	$CH_2CH(CH_3)_2$	$(CH_2)_2CH_3$	2.49	5.42	S
d	Phenyl	$(CH_2)_2CH_3$	4.11	1.68	S
e	Benzyl	$(CH_2)_2CH_3$	4.83	1.91	

For a, b, c, d and e, see the footnote to Table 1.

Acknowledgment. This work was supported by OCRC-KOSEF and basic science research program, Ministry of Education, Korea (BSRI-95-3410).

References

1. (a) Pirkle, W. H.; Hyun, M. H. *J. Org. Chem.* **1984**, *49*, 3043. (b) Pirkle, W. H.; McCune, J. E. *J. Chromatogr.* **1988**, *441*, 311. (c) Hyun, M. H.; Kim, M. H. *J. Liq. Chromatogr.* **1990**, *13*, 3229.
2. Pirkle, W. H.; Hyun, M. H.; Bank, B. *J. Chromatogr.* **1984**, *316*, 585.
3. (a) Pirkle, W. H.; Murray, P. G. *J. Chromatogr.* **1993**, *641*, 11. (b) Hyun, M. H.; Cho, S. M.; Ryoo, J.-J.; Kim, M. S. *J. Liq. Chromatogr.* **1994**, *17*, 317.
4. The detailed procedure of preparing CSP **1** and **5** by bonding chiral selector to 5 μm Rexchrom silica gel will be described elsewhere. Elemental analysis of CSP **1** (found : C, 6.43%; N, 1.14%) showed a loading of 0.23 mmol (based on C) or 0.20 mmol (based on N) of chiral selector per gram of stationary phase. Elemental analysis of CSP **5** (found : C, 4.51%; N, 0.88%) showed a loading of 0.17 mmol (based on C) or 0.16 mmol (based on N) of chiral selector per gram of stationary phase. CSP **1** and **5** prepared was packed into a 4.6 mm I.D.×250 mm stain-

less-steel HPLC column using a conventional slurry packing method.
5. The chromatographic results for resolving π-basic analytes on CSP **1** were similar to those on CSP **2**.
6. Pirkle, W. H.; Pochapsky, T. C. *Chem. Rev.* **1989**, *89*, 347.
7. Pirkle, W. H.; Finn, J. M.; Schreiner, J. L.; Hamper, B. C. *J. Am. Chem. Soc.* **1981**, *103*, 3964.
8. (a) Oi, N.; Nagase, M.; Doi, T. *J. Chromatogr.* **1983**, *257*, 111. (b) Pirkle, W. H.; Hyun, M. H. *J. Chromatogr.* **1985**, *322*, 309. (c) Hyun, M. H.; Whang, S.-R.; Ryoo, J.-J. *Chem. Letters* **1994**, 1021.
9. (a) Lienne, M.; Maccaudiere, P.; Caude, M.; Rosset, R.; Tambute, A. *Chirality* **1989**, *1*, 45. (b) Maccaudiere, P.; Lienne, M.; Caude, M.; Rosset, R.; Tambute, A. *J. Chromatogr.* **1989**, *467*, 357. (c) Hyun, M. H.; Min, C. S.; Cho, Y. J. *J. High Resoln Chromatogr.* **1995**, *18*, 63.

Photopolymerization of Methyl Methacrylate Initiated by CCl_4/Group VIII Metallocene

Hee-Gweon Woo*, Jin-Young Park, Lan-Young Hong, Soo-Yeon Yang, Hyun You, and Heui-Suk Ham

Department of Chemistry, Chonnam National University, Kwangju 500-757, Korea

Received January 18, 1996

Photopolymerization technology applicable conveniently is amply used on a commercial basis today in the areas of surface coatings, photoresists, adhesives, and holography.[1] Organometallic photochemistry has received a great amount of attention because irradiation of organometallics can lead to catalytically and synthetically useful transformations.[2] *Inter alia*, numerous cyclopentadienyl complexes, a historically important class of organometallics, have been prepared and their photochemical properties have been intensively investigated.[3] A number of halogenated organic compounds have been used as effective photoinitiators.[4] A practical problem with halogenated photoinitiators is the corrosion of reactor system caused by acid hydrogen halides which are produced as byproducts during the photopolymerization. The use of ferrocene (Cp_2Fe) as a photopolymerization catalyst (to activate the halogenated photoinitiator) and as a halide-radical trap (to prevent the troublesome acid formation) in combination with halogenated compounds has been reported.[5] To our knowledge, the other group VIII metallocenes such as cobaltocene (Cp_2Co) and nickelocene (Cp_2Ni) have never been used for this type of photopolymerization. Here we wish to report the photopolymerization of methyl methacrylate (MMA) initiated by CCl_4/group VIII metallocene.

In a typical experiment, a quartz test tube (1 cm×20 cm) charged with MMA (2.14 mL, 20 mmol), CCl_4 (0.19 mL, 2 mmol), Cp_2Fe (0.37 mg, 2 μmol), and benzene (2 mL) was degassed, sealed, and irradiated with 300 nm UV-light (monochromatic UV lamp intensity, 6.93×10^{18} hv mL^{-1} min^{-1}) for 2h. The polymer was precipitated in hexane, filtered off, and dried under reduced pressure to give 0.44 g (22%) of white solid.[6] Cobaltocene and nikelocene instead of ferrocene were also used with CCl_4 for the photopolymerization. Other halocarbons such as $CHCl_3$ and $Ph(C=O)CH_2Br$ were examined as a possible substitute for CCl_4. The results are summarized in Table 1.

Table 1. GPC Characterization of Photopolymerization of MMA[a]

Initiator	Yield (%)	mol wt[b]		
		M_w	M_n	PDI[c]
CCl_4+Cp_2Fe	22	110600	55700	2.0
CCl_4+Cp_2Co	3	232000	103300	2.3
CCl_4+Cp_2Ni	11	180600	84900	2.1
$CHCl_3+Cp_2Fe$	10	–	–	–
$Ph(C=O)CH_2Br+Cp_2Fe$	0	–	–	–
Cp_2Fe	trace	–	–	–
CCl_4	trace	–	–	–

[a]UV-irradiation for 2 h. [b]Measured with GPC in THF. [c]Polydispersity Index, M_w/M_n.

We used monomer : halide : metallocene with a fixed mole ratio of 10000 : 1000 : 1. We are studying their relative concentration effect on the photopolymerization and will be reported as a separate paper in the future. Fujisaki *et al.* suggested that the photopolymerization of MMA may be initiated by ferrocene/CCl_4 system as follows:[5b]

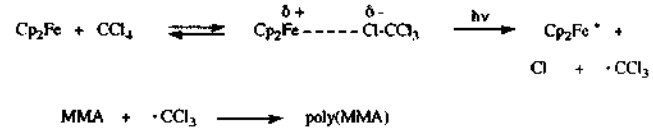

A charge-transfer (CT) complex formed between ferrocene and CCl_4 by the iron atom serving as an electron donor and the chlorine atom as an electron acceptor. The primary process of photochemical initiation of the polymerization could be the absorption of light by this CT complex which will then dissociate into trichloromethyl radical and ferricenium chloride. The trichloromethyl radical will finally initiate the photopolymerization. The CT complex formation seems to be a mandatory condition for the photopolymerization. As a control experiment, ferrocene or CCl_4 alone is practically ineffective on the photopolymerization. As shown in Table 1, $Ph(C=O)CH_2Br$ was ineffective because of inability of forming the CT complex with ferrocene. $CHCl_3$ was found to be less effective than CCl_4 (polymerization yield 10% *vs.* 22%). Radicals are particularly strongly stabilized when both an electron-withdrawing and an electron-donating substituent are located at the radical site.[7] Chlorine atom on the radical site could be more stabilizing the corresponding radical than hydrogen atom. Furthermore, the C-Cl bond dissociation energy in CCl_4 (84 kcal/mol) is smaller than the C-H bond dissociation energy (96 kcal/mol) in $CHCl_3$.[8] Such arguments were recently supported by the worldwide replacement of chlorofluorocarbons (CFCs) by hydrochlorofluorocarbons (HCFCs) because of ozone depletion in winter.[9]